Atmospheric Environment xxx (2011) 1–10

Contents lists available at SciVerse ScienceDirect

Atmospheric Environment

journal homepage: www.elsevier.com/locate/atmosenv

Annual sulfur deposition through fog, wet and dry deposition in the Kinki Region of Japan

Hikari Shimadera*, Akira Kondo, Kundan Lal Shrestha, Akikazu Kaga, Yoshio Inoue

Division of Sustainable Energy and Environmental Engineering, Graduate School of Engineering, Osaka University, 2-1 Yamadaoka, Suita, Osaka 565-0871, Japan

ARTICLE INFO

Article history:
Received 17 March 2011
Received in revised form
17 August 2011
Accepted 19 August 2011

Keywords:
Fog deposition
Acid deposition
Transboundary air pollution
WRF/CMAQ
Fog water deposition model

ABSTRACT

This study estimated annual sulfur ($SO_2 + SO_4^{2-}$) deposition through fog, wet and dry deposition in the Kinki Region of Japan from April 2004 to March 2005. The numerical models used in this study include the Weather Research and Forecasting model (WRF), the Community Multiscale Air Quality model (CMAQ), and a fog deposition model. WRF well predicted mountain fog at Mt. Rokko, the meteorology near the ground surface in the Kinki Region and the upper air meteorology in Japan during the simulation period. CMAQ well predicted the long-range atmospheric transport of aerosol SO_4^{2-} from the Asian Continent to Japan. The mean SO_4^{2-} concentration in fog water was approximately 6 times higher than that in precipitation in the Kinki Region. Ratios of fog water deposition to precipitation reached up to more than 10% in some mountainous areas in the Kinki Region. Consequently, the amount of sulfur deposition through fog water deposition was larger than that through dry deposition and comparable to that through wet deposition in some mountainous areas in the Kinki Region.

1. Introduction

Fog is a cloud on the ground surface and reduces the horizontal visibility to less than 1000 m. Fog can be classified into several types, such as radiation fog and mountain fog, in accordance with the formation mechanism. Radiation fog occurs through radiative cooling of humid air masses typically from night to early in the morning on flat terrains and in valleys. Mountain fog mainly occurs through orographic lifting of humid air masses or horizontal advection of low-level cloud to mountain ranges (Klemm et al., 2005).

Fog can affect forest ecosystems in mountainous areas, in which fog occurs more frequently than in other areas. Fog water deposition through the interception of fog droplets by vegetation can be an important part of the hydrologic budget of forests (Vong et al., 1991; Dawson, 1998). Ionic concentrations in fog water are much higher than those in rain water (Igawa et al., 1998; Aikawa et al., 2001). Consequently, fog can contribute significantly to atmospheric deposition in mountainous forest areas (Baumgardner et al., 2003; Klemm and Wrzesinsky, 2007). The effects of fog may be more pronounced in Japan than in other regions because approximately two-thirds of the land area are covered with forests, most of which are located in mountainous regions.

The amounts of fog water deposition have been measured using various approaches, such as the through fall measurement (e.g., Shubzda et al., 1995; Lange et al., 2003) and the eddy covariance method (e.g., Burkard et al., 2003; Klemm et al., 2005; Eugster et al., 2006). Numerical models also have been utilized to estimate fog water deposition. A one-dimensional model developed by Lovett (1984) has been widely used to predict fog water deposition in various mountain forests (e.g., Miller et al., 1993; Herckes et al., 2002a; Baumgardner et al., 2003). Katata et al. (2008) also developed a one-dimensional land surface model to better predict fog water deposition, and showed the model agreed better with the measurement data by Klemm et al. (2005) than the model developed by Lovett (1984).

The study of fog on a spatial scale requires numerical simulations because few fog monitoring sites exist and fog is highly variable according to regions. Mesoscale meteorological models have been employed for regional forecasting of particular fog events (e.g., Ballard et al., 1991; Pagowski et al., 2004). Shimadera et al. (2008) applied the 5th generation Mesoscale Model (MM5) (Grell et al., 1994) to fog simulation for months in the Kinki Region of Japan, and showed that the model well reproduced occurrence of fog. Shimadera et al. (2009) utilized MM5 and the Community Multiscale Air Quality model (CMAQ) (Byun and Ching, 1999) to predict concentrations of acidic compounds in fog water in the Kinki Region in March 2005. Shimadera et al. (2010) developed a two-dimensional fog water deposition model, and showed that the model was applicable to the estimate of spatial distribution of fog deposition with the meteorology and air quality modeling system.

* Corresponding author. Tel./fax: +81 06 6879 7670.
E-mail addresses: shimadera@ea.see.eng.osaka-u.ac.jp, simadera@criepi.denken.or.jp (H. Shimadera).

1352-2310/$ – see front matter © 2011 Elsevier Ltd. All rights reserved.
doi:10.1016/j.atmosenv.2011.08.055

The present study utilized the Weather Research and Forecasting model (WRF) (Skamarock et al., 2008), CMAQ and the fog deposition model in order to estimate annual sulfur ($SO_2 + SO_4^{2-}$) deposition through fog (not included in wet deposition in this study), wet and dry deposition in the Kinki Region of Japan from April 2004 to March 2005.

2. Numerical models

2.1. Meteorology and air quality modeling system

Meteorology and air quality models used in the present study are WRF version ARW 3.2.1 and CMAQ version 4.7.1. WRF is a three-dimensional, nonhydrostatic, terrain-following sigma-pressure coordinate mesoscale model with a multiple-nest capability, several physics options, and a four-dimensional data assimilation capability. CMAQ is a three-dimensional Eulerian air quality modeling system that simulates the transport, transformation, and dry and wet deposition of various air pollutants and their precursors across spatial scales ranging from local to hemispheric. For the present study, CMAQ was modified to output ionic concentrations in fog (cloud water at the first layer). The following relationship between the horizontal visibility (x_{vis}) (m) and the liquid water content of fog (LWC) (g m^{-3}) obtained from Stoelinga and Warner (1999) was utilized to judge whether fog occurred or not:

$$x_{vis} = -1000 \times \frac{\ln(0.02)}{144.7 LWC^{0.88}}. \quad (1)$$

It was considered that fog occurred when $x_{vis} < 1000$ m, i.e. $LWC > 0.017$ g m^{-3} at the first layer.

The WRF/CMAQ modeling system was run for the period from April 2004 to March 2005 with an initial spin-up period of March 2004. Fig. 1 shows modeling domains for CMAQ prediction. The study region is centered at (122.5°E, 32.5°N) on the Lambert conformal conic projection map of Asia. The horizontal domains consist of 4 domains from domain 1 (D1) covering a wide area of Asia to domain 4 (D4) covering most of the Kinki Region of Japan. The horizontal resolutions and the number of grid cells in the domains are 81, 27, 9 and 3 km, and 128 × 96, 66 × 66, 69 × 69 and 72 × 72 for D1, domain 2 (D2), domain 3 (D3) and D4, respectively. The vertical layers for the WRF and CMAQ predictions consist of 24 and 16 sigma-pressure coordinated layers from the surface to 100 hPa, respectively. The middle heights of the first, second and third layers are approximately 15, 50, and 110 m, respectively.

The observation data used for the WRF/CMAQ evaluations were obtained from fog sampling by the Hyogo Prefectural Government on Mt. Rokko, surface meteorological observation in D4 and upper air meteorological observation in Japan conducted by the Japan Meteorological Agency (JMA), air pollution monitoring by the Osaka Prefectural Government, and acid deposition monitoring by the Ministry of the Environment (MOE) of Japan. The locations of the observation sites are shown in Fig. 1. The fog sampling on Mt. Rokko was performed by using an active fog collector with a net consisting of Teflon string. The liquid water content of fog was estimated from volume of sampled fog water, sampling time, sampling flow rate, and collection efficiency. The concentrations of

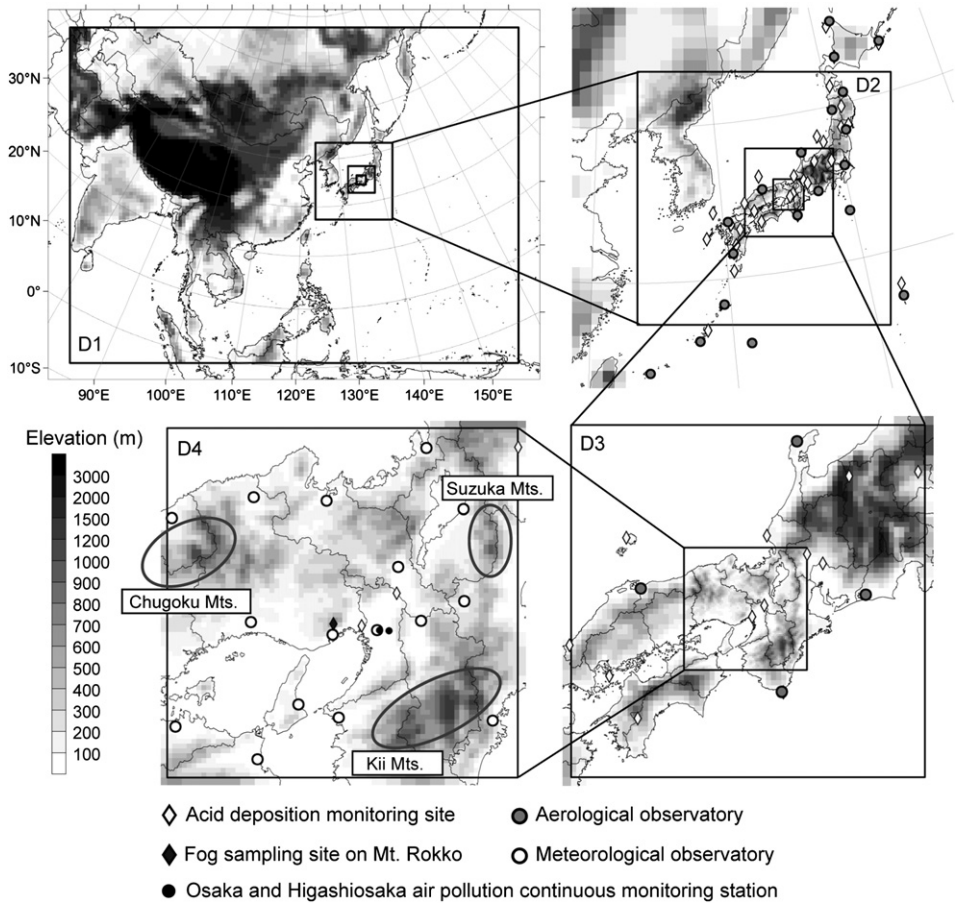

Fig. 1. Modeling domains for CMAQ prediction and locations of observation sites.

Please cite this article in press as: Shimadera, H., et al., Annual sulfur deposition through fog, wet and dry deposition in the Kinki Region of Japan, Atmospheric Environment (2011), doi:10.1016/j.atmosenv.2011.08.055

chemical species of sampled fog water were measured with an ion chromatograph. The details of the method are described in Aikawa et al. (2005).

For the meteorological prediction, WRF was configured with the Kain-Fritsch scheme (Kain, 2004) for the cumulus parameterization of D1–D3, the Yonsei University scheme (Hong et al., 2006) for planetary boundary layer parameterization, the WRF single-moment 3-class microphysics scheme (Hong et al., 2004; Hong and Lim, 2006), the Noah land surface model (Chen and Dudhia, 2001), the rapid radiative transfer model (Mlawer et al., 1997) for the long wave radiation and the scheme of Dudhia (1989) for the shortwave radiation simulations. Input data for WRF include the National Centers for Environmental Prediction final analysis (NCEP FNL) data, and the grid point value derived from the mesoscale model (GPV MSM) data by JMA. Initial and lateral boundary conditions for WRF were obtained from the NCEP FNL for D1 and the GPV MSM for D2. The WRF simulations from D2 to D4 were conducted with two-way nesting. Three-dimensional analysis nudging was applied to the west–east and north–south wind components in D1 and D2 with the nudging coefficient set to 3.0^{-5} s^{-1} for the entire simulation period.

For the air quality prediction, CMAQ was configured with the Statewide Air Pollution Research Center version 99 (SAPRC99) (Carter, 2000) mechanism for the gas-phase chemistry, the 5th generation CMAQ aerosol module (U.S. EPA, 2008) for the aerosol processes, and the cloud and aqueous phase chemistry option based on Chang et al. (1987) and Pleim and Chang (1992). The hourly results of WRF were processed using the Meteorology–Chemistry Interface Processor (MCIP) version 3.6. Initial and boundary conditions for D1 were obtained from the CMAQ default concentration profiles.

Emission data applied in this study include anthropogenic, biogenic volatile organic compounds (BVOC), biomass burning and volcanic SO_2 emissions. Anthropogenic and BVOC emissions for the Japan region were derived from an emissions inventory for Japan in the year 2000 called EAGrid2000-Japan (Kannari et al., 2007). For the other South and East Asia regions, anthropogenic emissions were obtained from an emissions inventory for Asia in the year 2006 developed by Zhang et al. (2009). Emissions of NH_3 were derived from predicted values for the year 2004 and 2005 of the regional emission inventory in Asia (Ohara et al., 2007). BVOC and biomass burning emissions were derived from Murano (2006) and Streets et al. (2003), respectively. For the other regions in D1, anthropogenic and biomass burning emissions were obtained from an emissions inventory prepared for Arctic Research of the Composition of the Troposphere from Aircraft and Satellites (http://mic.greenresource.cn/arctas_premission), and BVOC emissions were derived from Guenther (1995). The volcanic SO_2 emissions were obtained from Andres and Kasgnoc (1998) for volcanoes erupting continuously, and observation data by JMA for Miyakejima located to the south of Tokyo. Emissions from international shipping estimated by Corbett and Koehler (2003, 2004) were allocated with the ship emissions allocation factor by Wang et al. (2008).

To estimate the contribution of the transboundary air pollution from the other regions to Japan, the CMAQ simulations were conducted in two emission cases. The first is a baseline emission case with the total emissions described above (EB), and the other is an emission case where anthropogenic emissions in the land areas except Japan are set to be 0 (EJ). Fig. 2 shows spatial distributions of SO_2 emission rates in EB. The total emissions of SO_2 in EB and EJ are 57.1 and 7.5 Tg $year^{-1}$, respectively.

2.2. Fog deposition model

The fog water deposition model used in the present study is based on the two-dimensional model developed by Shimadera et al. (2010). The study showed that the model-predicted fog deposition velocity increased with increasing horizontal wind speed, and considerably varied with forest parameters. Moreover, the model-predicted fog deposition velocity was the largest at the windward edge of forest. It was also showed that the model well reproduced the deposition flux of mountain fog observed by Eugster et al. (2006).

Equations to simulate turbulent airflow in and above a forest canopy are based on equations used by Yamada (1982). An equation of mean motion is

$$\frac{\partial U}{\partial t} = \frac{\partial}{\partial z}\left(K_M \frac{\partial U}{\partial z}\right) - C_D A_S U|U|, \tag{2}$$

where U is the horizontal wind component (m s^{-1}), K_M is the eddy diffusivity of momentum (m^2 s^{-1}), C_D is the drag coefficient for a forest canopy and A_S is the one-sided surface area density (m^2 m^{-3}). The vertical distribution of A_S was obtained from a function proposed by Kondo and Akashi (1976).

An advection–diffusion equation of fog is

$$\frac{\partial LWC}{\partial t} = -\mathbf{U}\cdot\nabla LWC + \nabla(K_H \cdot \nabla LWC) - S_{IM} - S_S, \tag{3}$$

where K_H is the eddy diffusivity of heat (m^2 s^{-1}), S_{IM} and S_S are respectively fog water deposition terms by inertial impaction and gravitational settling of fog droplets on leaves. Inertial impaction is generally the dominant deposition mechanism, but gravitational settling can be important under low wind speed conditions (Lovett, 1984). K_M and K_H were obtained with the closure model of Mellor and Yamada (1982). S_{IM} and S_S are given by

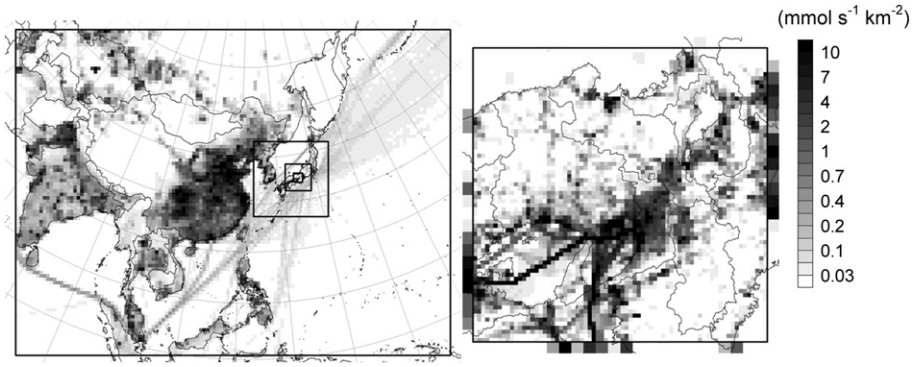

Fig. 2. Spatial distribution of annual mean SO_2 emission rate in EB.

Please cite this article in press as: Shimadera, H., et al., Annual sulfur deposition through fog, wet and dry deposition in the Kinki Region of Japan, Atmospheric Environment (2011), doi:10.1016/j.atmosenv.2011.08.055

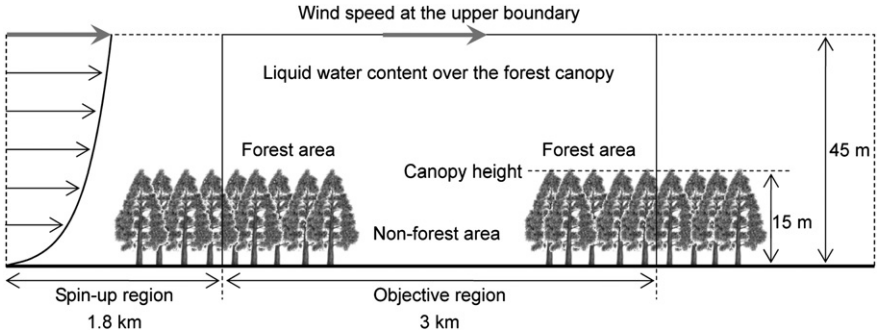

Fig. 3. Modeling domain for two-dimensional fog deposition model.

$$S_{IM} = A_L k_x \varepsilon_{IM} |U| LWC, \quad (4)$$

$$S_s = A_L k_z v_s LWC, \quad (5)$$

where A_L is the one-sided leaf area density ($m^2\ m^{-3}$), ε_{IM} is the efficiency of inertial impaction, v_S is the gravitational settling velocity of fog droplets, k_x and k_z are respectively the portions of the effective leaf area for deposition of fog droplets by inertial impaction and gravitational settling. The efficiencies of inertial impaction ε_{IM} for needle and broad leaves were obtained with an empirical function proposed by Katata et al. (2008). The gravitational settling velocity v_S is given by

$$v_s = \frac{g d_p^2 (\rho_W - \rho_A)}{18 \mu_A}, \quad (6)$$

where g is the acceleration of gravity ($m\ s^{-2}$), d_p is the volume-weighted mean diameter of fog droplet (m), ρ_W and ρ_A are respectively the densities of liquid water and air ($kg\ m^{-3}$), and μ_A is the viscosity coefficient of air ($kg\ m^{-1}\ s^{-1}$). Droplet size of fog can be expressed as a function of *LWC* (e.g., Eugster et al., 2006; Katata et al., 2008). Because of lack of observation data on droplet size of fog in the study region, this study utilized the observation data by Burkard et al. (2003) at the Lägeren research site in Switzerland to obtain the following relationship between d_p and *LWC*:

$$d_P = \left(11.6 LWC^{0.305} + 15.8 LWC + 4.0\right) \times 10^{-6}. \quad (7)$$

According to Petroff et al. (2009), k_x and k_z are expressed by

$$k_x = \int_{\theta_L=0}^{2/\pi} \int_{\phi_L=0}^{2\pi} \varphi_{\theta_L} \varphi_{\phi_L} \sin\theta_L |\cos\phi_L| \mathrm{d}\theta_L \mathrm{d}\phi_L, \quad (8)$$

$$k_z = \int_{\theta_L=0}^{2/\pi} \varphi_{\theta_L} \cos\theta_L \mathrm{d}\theta_L, \quad (9)$$

$$\varphi_{\theta_L}(\alpha_L) = \frac{2}{\pi} \frac{\Gamma(\mu_L + \nu_L)}{\Gamma(\mu_L)\Gamma(\nu_L)} \left(1 - \frac{2\alpha_L}{\pi}\right)^{\mu_L - 1} \left(\frac{2\alpha_L}{\pi}\right)^{\nu_L - 1}, \alpha_L \in \left[0; \frac{2}{\pi}\right], \quad (10)$$

$$\varphi_{\phi_L}(\alpha_L) = \frac{1}{2\pi}, \ \alpha_L \in [0; 2\pi], \quad (11)$$

where θ_L and ϕ_L are respectively the inclination and azimuth of leaves, φ_{θ_L} and φ_{ϕ_L} are the leaf angular densities associated with each angle, Γ is the Euler Gamma-function, μ_L and ν_L are parameters depending on the canopy species, location and time. For simplification, it was assumed that all leaf orientations were equi-probable, i.e., μ_L and ν_L were set to be 1.

Fig. 3 shows the modeling domain for the fog deposition model. The width of the objective region is set to 3 km for predictions of fog water deposition in 3-km grid cells in D4. Horizontal and vertical resolutions are 60 and 1 m, respectively. Forest areas are allocated to the objective region from its edges according to forest fraction. Spatial distribution of forest fractions in D4 was obtained from the 100-m land use dataset of the Digital National Land Information in Japan (http://nlftp.mlit.go.jp/ksj/). Forest areas cover 69% of the land areas and 95% of the mountainous areas with elevation ≥500 m in D4. Spatial distributions of leaf area index (LAI) in D4 were derived from the global datasets of monthly 1-km LAI with the Moderate resolution imaging spectroradiometer (MODIS) (http://cliveg.bu.edu/modismisr/index.html). Mean values of LAI in the forest areas in D4 are 2.5 in the spring (April and May 2004, and March 2005), 2.8 in the summer (June, July and August 2004), 2.2 in the fall (September, October and November 2004) and 1.4 in the winter (December 2004, January and February 2005). Spatial

Table 1
Statistical performance for meteorological predictions near the ground surface at the meteorological observatories in D4 and at 925 hPa surface above the aerological observatories in Japan from April 2004 to March 2005.

		Surface	925 hPa
Temperature	Sample number	139823 (8625–8760)	14580 (714–730)
	Mean Obs. (°C)	16.4 (15.2–17.7)	11.8 (2.8–19.3)
	Mean WRF (°C)	16.2 (14.2–17.8)	11.3 (1.3–18.5)
	MAE (°C)	1.6 (1.2–1.8)	1.2 (0.9–2.9)
	IA	0.99 (0.97–0.99)	0.99 (0.95–1.00)
Humidity	Sample number	139970 (8637–8760)	14574 (710–730)
	Mean Obs. ($g\ kg^{-1}$)	9.0 (8.3–9.9)	8.4 (4.3–12.4)
	Mean WRF ($g\ kg^{-1}$)	9.1 (8.6–9.9)	8.6 (4.5–13.3)
	MAE ($g\ kg^{-1}$)	0.9 (0.8–1.0)	1.1 (0.7–1.9)
	IA	0.98 (0.98–0.99)	0.98 (0.75–0.98)
Wind speed	Sample number	138868 (8467–8752)	14526 (714–730)
	Mean Obs. ($m\ s^{-1}$)	2.8 (1.5–4.2)	8.6 (7.0–10.7)
	Mean WRF ($m\ s^{-1}$)	3.9 (2.5–4.9)	9.0 (6.8–10.3)
	RMSE ($m\ s^{-1}$)	2.5 (1.4–3.4)	3.2 (2.2–5.0)
	IA	0.70 (0.41–0.83)	0.90 (0.73–0.94)
Wind U-component	Sample number	138868 (8467–8752)	14526 (714–730)
	Mean Obs. ($m\ s^{-1}$)	0.4 (−0.3–0.9)	1.7 (−3.6–5.3)
	Mean WRF ($m\ s^{-1}$)	0.7 (−0.3–1.4)	1.6 (−4.8–6.4)
	RMSE ($m\ s^{-1}$)	2.5 (1.6–3.0)	3.3 (2.2–4.9)
	IA	0.77 (0.53–0.87)	0.95 (0.82–0.97)
Wind V-component	Sample number	138868 (8467–8752)	14526 (714–730)
	Mean Obs. ($m\ s^{-1}$)	−0.3 (−0.8–0.3)	0.1 (−1.5–1.7)
	Mean WRF ($m\ s^{-1}$)	−0.2 (−1.0–0.6)	−0.2 (−3.0–1.8)
	RMSE ($m\ s^{-1}$)	2.6 (1.8–2.8)	3.4 (2.8–4.4)
	IA	0.78 (0.52–0.89)	0.93 (0.79–0.97)
Precipitation	Annual Obs. (mm)	2135 (1458–5316)	
	Annual WRF (mm)	1893 (1169–3505)	

Parenthetical values show ranges of values at the individual observatories.

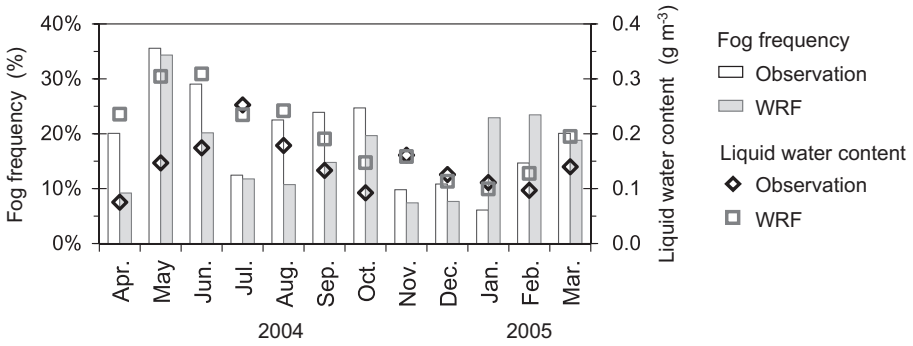

Fig. 4. Observed and WRF-predicted monthly fog frequency and mean liquid water content of fog at the Mt. Rokko fog sampling site from April 2004 to March 2005.

distribution of tree species in D4 was obtained from the 1-km vegetation dataset of the 5th National Survey on the Natural Environment in Japan (http://www.biodic.go.jp/kiso/fnd_f.html). Needle-leaved and broad-leaved forest areas account for 69 and 31% of the total forest area in D4, respectively. Height of the forest canopy was assumed to be 15 m. Meteorological input data, including the wind speed at the upper boundary and the liquid water content over the forest canopy, were derived from the WRF predictions at the first and second layers. Although the chemical composition of fog droplets can vary with droplet size (Herckes et al., 2002b; Fahey et al., 2005), CMAQ can predict only the bulk aqueous phase chemistry. In this study, hourly sulfur deposition through fog was estimated though multiplication of the model-predicted fog water deposition by the CMAQ-predicted concentrations in fog.

3. Results of meteorology and air quality predictions

3.1. Meteorology prediction

The performance for WRF predictions was evaluated using the mean absolute error (MAE), the root mean square error (RMSE) and the index of agreement (IA) (Willmott, 1981). The statistical measures are defined as

$$\mathrm{MAE} = \frac{1}{N}\sum_{i=1}^{N}|M_i - O_i|, \tag{12}$$

$$\mathrm{RMSE} = \left[\frac{1}{N}\sum_{i=1}^{N}(M_i - O_i)^2\right]^{\frac{1}{2}}, \tag{13}$$

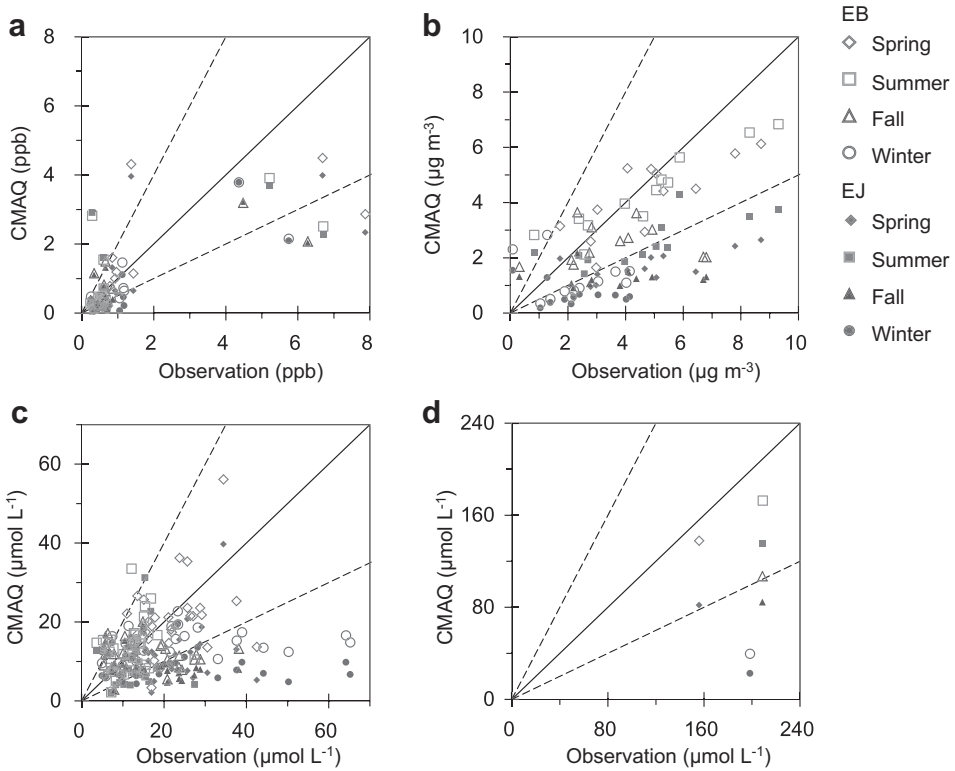

Fig. 5. Scatter plots of the observed versus CMAQ-predicted seasonal mean concentrations of (a) SO_2, (b) aerosol SO_4^{2-}, (c) SO_4^{2-} in precipitation and (d) SO_4^{2-} in fog for the period from April 2004 to March 2005 at the individual observation sites. 2:1, 1:2 and 1:1 reference lines are provided.

Please cite this article in press as: Shimadera, H., et al., Annual sulfur deposition through fog, wet and dry deposition in the Kinki Region of Japan, Atmospheric Environment (2011), doi:10.1016/j.atmosenv.2011.08.055

Table 2
CMAQ-predicted seasonal and annual mean concentrations of sulfur compounds in the land areas in EB-D4 from April 2004 to March 2005.

	Spring	Summer	Fall	Winter	Annual
SO_2 (ppb)	1.7 (22)	1.1 (0)	1.1 (8)	0.8 (18)	1.2 (12)
Aerosol SO_4^{2-} (μg m^{-3})	4.5 (61)	4.5 (32)	2.8 (47)	0.8 (46)	3.1 (47)
SO_4^{2-} in precipitation (μmol L^{-1})	21 (38)	20 (16)	13 (21)	13 (36)	16 (28)
SO_4^{2-} in fog (μmol L^{-1})	125 (43)	127 (31)	84 (30)	30 (29)	94 (35)

Parenthetical values are corresponding contribution rates of transboundary air pollution (%).

$$\mathrm{IA} = 1 - \frac{\sum_{i=1}^{N}(M_i - O_i)^2}{\sum_{i=1}^{N}(|M_i - \overline{O}| + |O_i - \overline{O}|)^2}, \quad (14)$$

where $\overline{M}$ and $\overline{O}$ are mean model-predicted and observed values, M_i and O_i are model-predicted and observed values, and N is the number of samples, respectively. Emery et al. (2001) set benchmarks with the statistical measures for the meteorology model performance: MAE $\leq$ 2 °C and IA $\geq$ 0.8 for temperature, MAE $\leq$ 2 g kg^{-1} and IA $\geq$ 0.6 for humidity, RMSE $\leq$ 2 m $s^{-1}$and IA $\geq$ 0.6 for wind speed.

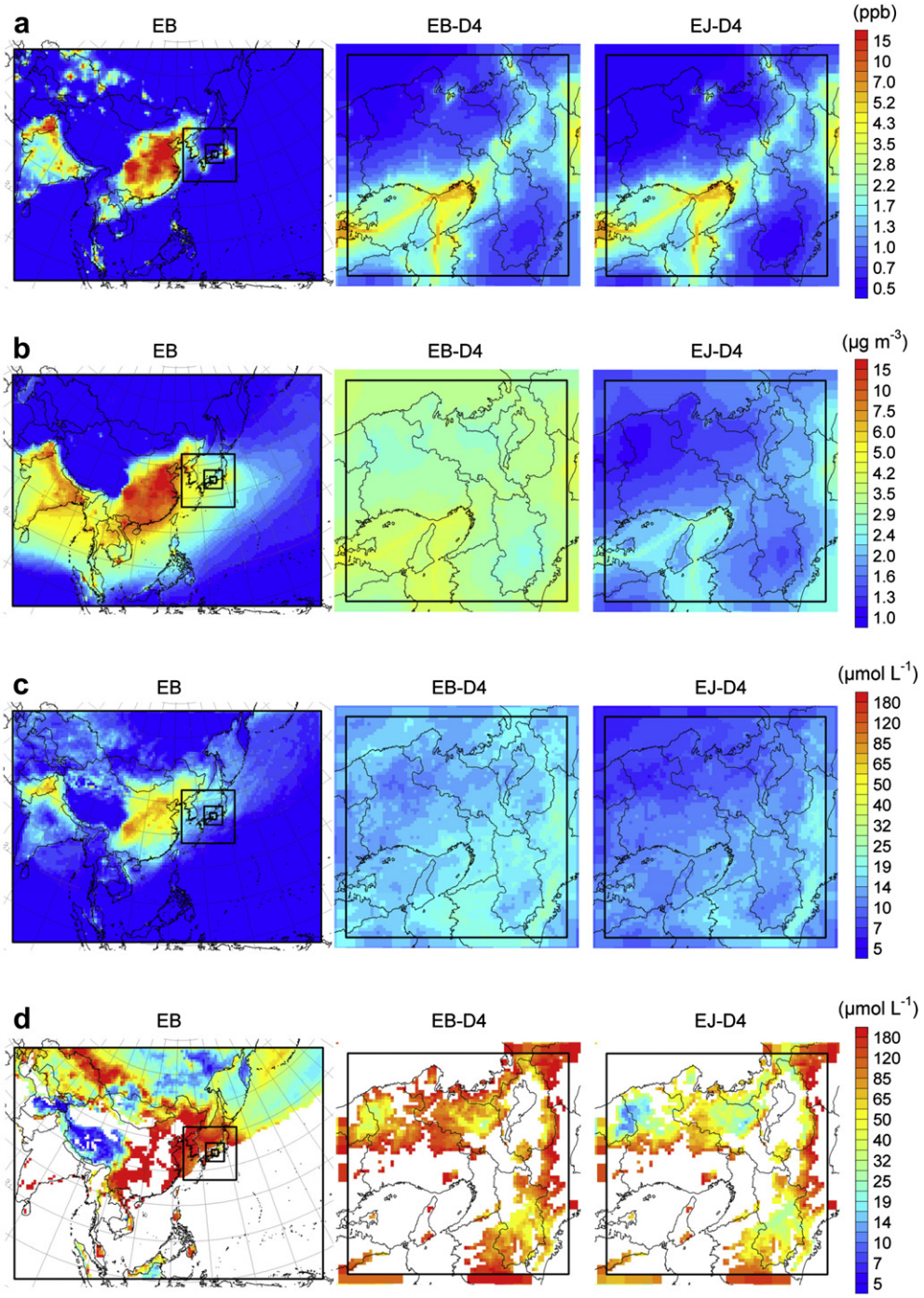

Fig. 6. Spatial distributions of CMAQ-predicted annual mean concentrations of (a) SO_2, (b) aerosol SO_4^{2-}, (c) SO_4^{2-} in precipitation and (d) SO_4^{2-} in fog from April 2004 to March 2005. The results of SO_4^{2-} concentrations in fog are not shown in grid cells with fog frequencies <2%.

Please cite this article in press as: Shimadera, H., et al., Annual sulfur deposition through fog, wet and dry deposition in the Kinki Region of Japan, Atmospheric Environment (2011), doi:10.1016/j.atmosenv.2011.08.055

Table 3
Model-predicted seasonal and annual fog frequency, liquid water content of fog, fog water deposition and precipitation in the land areas in D4 from April 2004 to March 2005.

	Elevation	Spring	Summer	Fall	Winter	Annual
Fog frequency (%)	500 m <	2.2	1.8	0.7	3.5	2.1
	≥500 m	13.5	12.4	10.1	20.9	14.2
Liquid water content (g m^{-3})	500 m <	0.14	0.13	0.09	0.13	0.15
	≥500 m	0.18	0.21	0.17	0.11	0.16
Fog water deposition (mm)	500 m <	3	3	1	1	8
	≥500 m	35	50	29	16	129
Precipitation (mm)	500 m <	522	386	723	482	2113
	≥500 m	784	833	1085	832	3533

Table 1 summarizes WRF performance for meteorological predictions near the ground surface at the meteorological observatories in D4 and at 925 hPa surface above the aerological observatories in Japan from April 2004 to March 2005. For temperature and humidity near the ground surface, the WRF predictions met the benchmarks for MAE and IA at all the meteorological observatories. The results indicate that WRF well captured variations in temperature and humidity associated with changes of seasons and synoptic scale factors such as passages of low pressure systems. For wind near the ground surface, while the WRF predictions met the benchmark for IA, the model performance was inferior to that for temperature and humidity. This may be attributed to the difficulty in predictions of weak and variable winds near the ground surface. Results of meteorology predictions in some other studies also indicated such tendencies (e.g., Gilliam et al., 2006; Lee et al., 2007). For wind at the 925 hPa surface, however, the WRF predictions well agreed with the observations. For precipitation, WRF tended to underestimate the amounts at the meteorological observatories, but approximately captured the regional variations. Overall, WRF successfully simulated the meteorology fields from April 2004 to March 2005.

Fig. 4 shows observed and WRF-predicted monthly frequency of fog occurrence and mean liquid water content during fog events at the Mt. Rokko fog sampling site from April 2004 to March 2005. The WRF predictions approximately captured monthly variations of fog frequency and liquid water content. Consequently, the predicted annual values well agreed with the observed ones, with the observed and predicted annual fog frequencies being 19% and 17% and annual mean liquid water contents being 0.15 g m^{-3} and 0.21 g m^{-3}, respectively.

3.2. Air quality prediction

Fig. 5 shows scatter plots of the observed versus CMAQ-predicted seasonal mean concentrations of sulfur compounds from April 2004 to March 2005. The CMAQ-predicted concentrations in EB were generally higher and agreed better with the observations than those in EJ, indicating that the model well simulated the transboundary air pollution. While CMAQ tended to underpredict the concentrations in the winter, most of the predicted seasonal values in EB were approximately within a factor of 2 of the observations. The CMAQ performance for predictions of SO_4^{2-} concentrations in fog at Mt. Rokko was comparable to that in precipitation in Japan.

Table 2 summarizes CMAQ-predicted seasonal and annual mean concentrations of sulfur compounds in the land areas in EB-D4 and

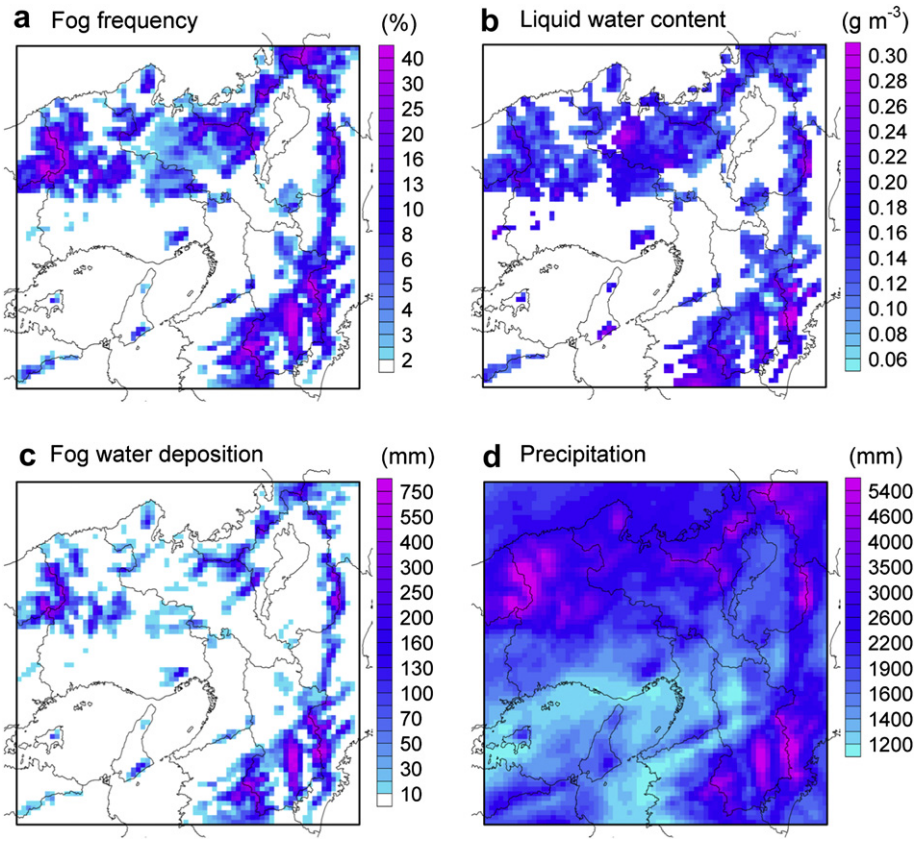

Fig. 7. Spatial distributions of model-predicted (a) fog frequency, (b) mean liquid water content of fog, (c) annual fog water deposition and (d) annual precipitation in D4 from April 2004 to March 2005. The results of liquid water content are not shown in grid cells with fog frequencies <2%.

Please cite this article in press as: Shimadera, H., et al., Annual sulfur deposition through fog, wet and dry deposition in the Kinki Region of Japan, Atmospheric Environment (2011), doi:10.1016/j.atmosenv.2011.08.055

Table 4
Model-predicted seasonal and annual sulfur deposition through dry, wet and fog deposition in the land areas in EB-D4 from April 2004 to March 2005.

	Elevation	Spring	Summer	Fall	Winter	Annual
Dry (mmol m^{-2})	500 m <	5.5 (21)	4.1 (1)	3.8 (10)	3.9 (23)	17.3 (14)
	≥500 m	6.1 (28)	3.6 (0)	4.4 (13)	3.3 (29)	17.3 (18)
Wet (mmol m^{-2})	500 m <	10.7 (37)	7.7 (16)	9.2 (20)	6.3 (35)	33.9 (27)
	≥500 m	16.8 (42)	15.9 (16)	14.0 (20)	11.0 (39)	57.6 (29)
Fog (mmol m^{-2})	500 m <	0.5 (42)	0.5 (34)	0.1 (28)	0.0 (26)	1.1 (37)
	≥500 m	4.2 (41)	4.7 (26)	2.3 (29)	0.4 (38)	11.6 (32)
Total (mmol m^{-2})	500 m <	16.6 (32)	12.3 (12)	13.1 (17)	10.3 (31)	52.3 (23)
	≥500 m	27.0 (39)	24.2 (15)	20.6 (19)	14.8 (36)	86.5 (27)

Parenthetical values are corresponding contribution rates of transboundary air pollution (%).

corresponding contribution rates of the transboundary air pollution from April 2004 to March 2005. Fig. 6 shows spatial distributions of the CMAQ-predicted annual mean concentrations of sulfur compounds for EB, EB-D4 and EJ-D4. The spatial distribution of mean SO_2 concentration in EB-D4 was similar to that in EJ-D4, particularly in and around the high SO_2 emission areas (Fig. 2). In the CMAQ prediction, transport of an air mass from East China to the Kinki Region of Japan generally took 2 days or more, which was equivalent to or longer than the atmospheric lifetime of SO_2 suggested in other studies (e.g., Restad et al., 1998; Tsai et al., 2010). These findings indicate the large contribution of local emissions and small contribution of the transboundary air pollution to SO_2 concentration in the Kinki Region. Large amounts of aerosol SO_4^{2-}, which were primarily produced through the oxidation of SO_2, were transported from the Asian Continent to Japan. Consequently, the transboundary air pollution contributed significantly to not only aerosol SO_4^{2-} concentration but also SO_4^{2-} concentration in precipitation and fog, particularly in the spring, in D4. The mean SO_4^{2-} concentration in fog was approximately 6 times higher than that in precipitation in the land areas in EB-D4. Aikawa et al. (2001) reported that the observed concentration of chemical species in fog was approximately 7 times higher than that in precipitation at the Mt. Rokko fog sampling site. The finding indicates that the result of this study is reasonable.

4. Fog water deposition in the Kinki Region

Table 3 summarizes model-predicted seasonal and annual fog frequency, liquid water content of fog, fog water deposition and precipitation in the land areas in D4 from April 2004 to March 2005. In order to show the importance of fog in high elevation areas, the land areas in D4 were classified into two zones: the land areas with elevation <500 m and the mountainous areas with elevation ≥500 m, which respectively accounted for 57 and 15% of D4. Fig. 7 shows spatial distributions of the model-predicted annual frequency of fog occurrence, liquid water content of fog, fog water deposition and precipitation in D4. Fog frequency, fog water deposition and precipitation generally increased with increasing elevation, with mean values of annual fog frequency, fog water deposition and precipitation in the mountainous areas with elevation ≥500 m being 6.9, 17 and 1.7 times larger than those in the land areas with elevation <500 m. The results indicate that effects of fog are much more variable from region to region than those of precipitation.

The values of fog frequency in wide areas of high mountains were comparable to or higher than those in Mt. Rokko, which is characterized by its high frequency of fog (Aikawa et al., 2001). In Kii Mts., Chugoku Mts. and Suzuka Mts. (Fig. 1), annual fog frequencies at individual 3-km grid cells reached up to 52, 49 and 43%, respectively.

Among the four seasons, the amounts of fog deposition was the largest in the summer due to large liquid water content and thick vegetation cover, and the smallest in the winter due to small liquid water content and thin vegetation cover. Seasonal mean fog water deposition velocities in the mountainous areas with elevation ≥500 m were 14, 15, 14 and 8.4 cm s^{-1} in the spring, summer, fall and winter. Impaction and gravitational settling of fog droplet respectively accounted for 94 and 6% of the total fog water deposition in D4, indicating that mountain fog events with relatively high wind speed dominantly contributed to fog water deposition. Annual ratio of fog water deposition to precipitation was only 1.1% in the entire D4, but was 3.7% in the mountainous areas with elevation ≥500 m. Moreover, in Mt. Rokko, Kii Mts., Chugoku Mts. and Suzuka Mts, annual ratios of fog water deposition to precipitation at individual 3-km grid cells reached up to 6.0, 16, 10 and 11%, respectively.

In other studies conducted in the temperate zone, observed turbulent fog water deposition velocities generally ranged from 0 to 10 cm s^{-1} at Speulderbos in the Netherlands (Vermeulen et al., 1997). Observed fog water deposition velocities generally ranged from 0 to 30 cm s^{-1} at the Waldstein research site in Germany (Klemm and Wrzesinsky, 2007). Model-predicted seasonal mean fog water deposition velocities ranged from 18 to 27 cm s^{-1} at Whiteface Mountain in the United States (Miller et al., 1993). Ratios of fog water deposition to precipitation in mountainous forests were 3.4% at the Lägeren research site in Switzerland (Burkard et al., 2003), 4.4% in Vosges Mts. in France (Herckes et al., 2002a), 9.4% at the Waldstein research site in Germany (Klemm and Wrzesinsky, 2007), 13–25% in the Southern Appalachian Region of the United States (Shubzda et al., 1995), and 22% at Whiteface Mountain in the United States (Miller et al., 1993), respectively. Although a direct comparison may not be appropriate given the differences in regions and methods, the results in this study are in the range of reported values in other studies.

5. Sulfur deposition in the Kinki Region

Table 4 summarizes the model-predicted seasonal and annual sulfur deposition through dry, wet and fog deposition in the land

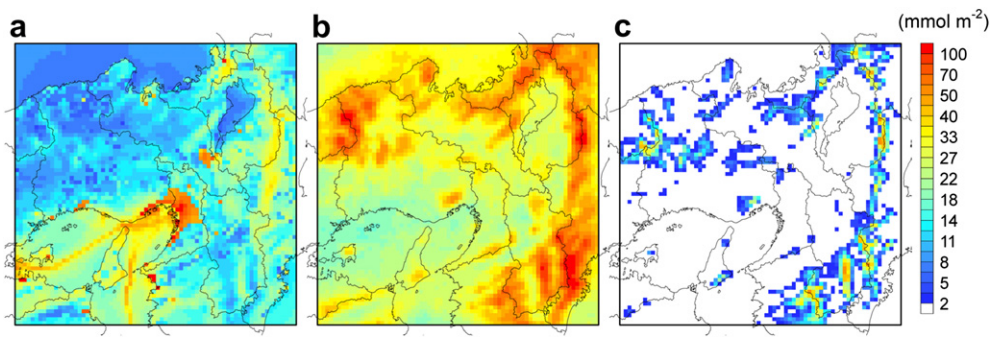

Fig. 8. Spatial distributions of model-predicted annual sulfur deposition through (a) dry, (b) wet and (c) fog deposition in EB-D4 from April 2004 to March 2005.

Please cite this article in press as: Shimadera, H., et al., Annual sulfur deposition through fog, wet and dry deposition in the Kinki Region of Japan, Atmospheric Environment (2011), doi:10.1016/j.atmosenv.2011.08.055

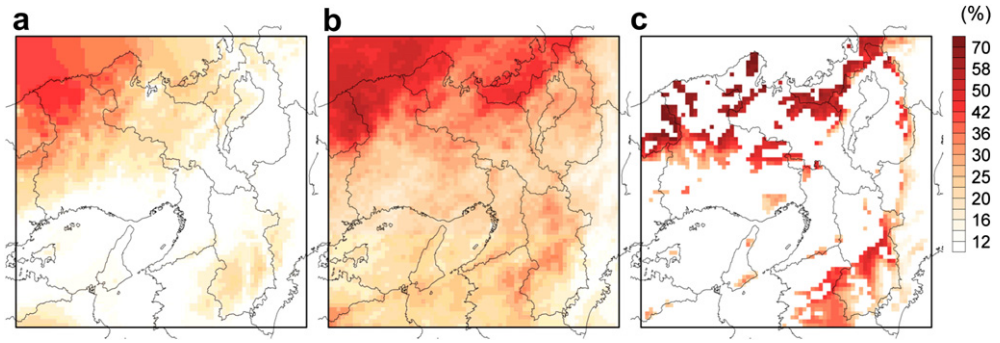

Fig. 9. Spatial distributions of model-predicted contribution rates of transboundary air pollution to annual sulfur deposition through (a) dry, (b) wet and (c) fog deposition from April 2004 to March 2005. The results for fog deposition are not shown in grid cells with corresponding annual sulfur deposition <2 mmol m^{-3}.

areas in EB-D4 and corresponding contribution rates of the transboundary air pollution from April 2004 to March 2005. Fig. 8 and Fig. 9 show spatial distributions of the model-predicted annual sulfur deposition through dry, wet and fog deposition in EB-D4 and those of corresponding contribution rate of the transboundary air pollution, respectively. The amount of dry deposition of SO_2 accounted for 75% of the total dry sulfur deposition in the land areas in EB-D4. Therefore, the amount of sulfur deposition through dry deposition was large in the high SO_2 emission areas (Fig. 2), and corresponding contribution of the transboundary air pollution was relatively small.

The contribution rates of the transboundary air pollution varied considerably from region to region, and were large in northern areas in D4. The transboundary air pollution contributed 6–57% of the total sulfur deposition at individual 3-km grid cells, and 24% in the entire D4. Ichikawa et al. (1998) and Lin et al. (2008) estimated that the transboundary air pollution contributed 42 and 31% of sulfur deposition in Japan in 1990 and 2001, respectively. The contribution rate in D4 in this study was smaller than those in Japan in these studies. The difference can be attributed to various reasons, such as differences in study years and regions, meteorology fields, emission data and model structures.

The amount of sulfur deposition through wet deposition was large in the mountainous areas since the amount of precipitation was also large in the mountainous areas (Fig. 7d). The sulfur deposition through wet deposition contributed the most to the total sulfur deposition among the three deposition processes, accounting for 64% the total sulfur deposition in the entire area in EB-D4.

The sulfur deposition through fog water deposition accounted for only 4.3% the total sulfur deposition in the entire area in EB-D4. In some mountainous areas, however, the amount of sulfur deposition through fog water deposition was larger than that through dry deposition and comparable to that through wet deposition. In Mt. Rokko, Kii Mts., Chugoku Mts. and Suzuka Mts, ratios of the sulfur deposition through fog to the total sulfur deposition at individual 3-km grid cells reached up to 24, 36, 31 and 31%, respectively. The results indicate that fog water deposition is an important atmospheric deposition process in mountainous forest areas in the Kinki Region of Japan.

6. Conclusions

The present study estimated annual sulfur deposition through fog, wet and dry deposition in the Kinki Region of Japan for the period from April 2004 to March 2005. The meteorology and air quality predictions were performed with the WRF/CMAQ modeling system in the 4 nested modeling domains from D1 covering a wide area of Asia to D4 covering most of the Kinki Region. WRF successfully simulated the meteorology near the ground surface in the Kinki Region and the upper air meteorology in Japan, and approximately captured mountain fog at the Mt. Rokko fog sampling site. CMAQ well predicted the long-range atmospheric transport of aerosol SO_4^{2-} from the Asian Continent to Japan, which strongly affected SO_4^{2-} concentrations in precipitation and fog in the Kinki Region. Mean SO_4^{2-} concentration in fog was approximately 6 times higher than that in precipitation in the Kinki Region.

The fog water deposition and corresponding sulfur deposition were estimated with the two-dimensional fog deposition model and the results of the WRF/CMAQ modeling system in the Kinki Region. Annual ratio of fog water deposition to precipitation was only 1.1% in the entire D4, but reached up to more than 10% in some mountainous areas with high fog frequencies, such as Kii Mts., Chugoku Mts. and Suzuka Mts.

The amount of sulfur deposition through dry deposition was large in the high SO_2 emission areas, and that through wet deposition was large in the mountainous areas due to the large amount of precipitation. The sulfur deposition through wet deposition contributed the most to the total sulfur deposition among the three deposition processes in the Kinki Region. The sulfur deposition through fog accounted for only 4.3% the total sulfur deposition in the entire D4. However, annual ratio of the sulfur deposition through fog to the total sulfur deposition reached up to more than 30% in some mountainous areas. The results indicate that fog water deposition is an important atmospheric deposition process in mountainous forest areas in the Kinki Region of Japan.

Acknowledgments

We are grateful to the Hyogo Prefectural Governments and MOE of Japan for providing the observation data associated with the WRF/CMAQ evaluations and to Dr. Werner Eugster for providing the observation data on fog water deposition by Burkard et al. (2003) and Eugster et al. (2006).

This work was supported by Grant-in-Aid for JSPS Fellows.

References

Aikawa, M., Hiraki, T., Shoga, M., Tamaki, M., 2001. Fog and precipitation chemistry at Mt. Rokko in Kobe, April 1997–March 1998. Water, Air, and Soil Pollution 130 (1–4), 1517–1522.

Aikawa, M., Hiraki, T., Shoga, M., Tamaki, M., 2005. Chemistry of fog water collected in the Mt. Rokko area (Kobe City, Japan) between April 1997 and March 2001. Water, Air, and Soil Pollution 160 (1–4), 373–393.

Andres, R.J., Kasgnoc, A.D., 1998. A time-averaged inventory of subaerial volcanic sulfur emissions. Journal of Geophysical Research D: Atmospheres 103 (D19), 25251–25261.

Ballard, S.P., Golding, B.W., Smith, R.N.B., 1991. Mesoscale model experimental forecasts of the haar of northeast Scotland. Monthly Weather Review 119, 2107–2123.

Baumgardner, R.E., Kronmiller, K.G., Anderson, J.B., Bowser, J.J., Edgerton, E.S., 2003. Estimates of cloud water deposition at mountain acid deposition program sites in the Appalachian Mountains. Atmospheric Environment 33 (30), 5105–5114.
Burkard, R., Butzberger, P., Eugster, W., 2003. Vertical fogwater flux measurements above an elevated forest canopy at the Lägeren research site. Switzerland Atmospheric Environment 37 (21), 2979–2990.
Byun, D.W., Ching, J.K.S. (Eds.), 1999. Science Algorithms of the EPA Models-3 Community Multi-scale Air Quality (CMAQ) Modeling System. NERL, Research Triangle Park, NC.
Carter, W.P.L., 2000. Documentation of the SAPRC-99 chemical mechanism for VOC reactivity assessment. Final Report to California Air Resources Board Contract No. 92-329, and (in part) pp. 95–308.
Chang, J.S., Brost, R.A., Isaksen, I.S.A., Madronich, S., Middleton, P., Stockwell, W.R., Walcek, C.J., 1987. A three-dimensional Eulerian acid deposition model: physical concepts and formulation. Journal of Geophysical Research 92 (D12), 14681–14700.
Chen, F., Dudhia, J., 2001. Coupling an advanced land-surface/hydrology model with the Penn State/NCAR MM5 modeling system—part I: model implementation and sensitivity. Monthly Weather Review 129 (4), 569–585.
Corbett, J.J., Koehler, H.W., 2003. Updated emissions from ocean shipping. Journal of Geophysical Research 108 (D20), 4650.
Corbett, J.J., Koehler, H.W., 2004. Considering alternative input parameters in an activity-based ship fuel consumption and emissions model: reply to comment by Øyvind Endresen et al. on "Updated emissions from ocean shipping". Journal of Geophysical Research 109 (D23), 1–8.
Dawson, T.E., 1998. Fog in the California redwood forest: ecosystem inputs and use by plants. Oecologia 117 (4), 476–485.
Dudhia, J., 1989. Numerical study of convection observed during the Winter Monsoon Experiment using a mesoscale two-dimensional model. Journal of the Atmospheric Sciences 46 (20), 3077–3107.
Emery, C., Tai, E., Yarwood, G., 2001. Enhanced meteorological modeling and performance evaluation for two texas ozone episodes. Prepared for The Texas Natural Resource Conservation Commission 12118 Park 35 Circle Austin, Texas 78753.
Eugster, W., Burkard, R., Holwerda, F., Scatena, F.N., Bruijnzeel, L.A.(S.), 2006. Characteristics of fog and fogwater fluxes in a Puerto Rican elfin cloud forest. Agricultural and Forest Meteorology 139 (3–4), 288–306.
Fahey, K.M., Pandis, S.N., Collett Jr., J.L., Herckes, P., 2005. The influence of size-dependent droplet composition on pollutant processing by fogs. Atmospheric Environment 39 (25), 4561–4574.
Gilliam, R.C., Hogrefe, C., Rao, S.T., 2006. New methods for evaluating meteorological models used in air quality applications. Atmospheric Environment 40 (26), 5073–5086.
Grell, G.A., Dudhia, J., Stauffer, D.R., 1994. A Description of the Fifth-Generation Penn State/NCAR Mesoscale Model (MM5) NCAR Technical Note NCAR/TN-398+STR, 117pp.
Guenther, A., 1995. A global model of natural volatile organic compound emissions. Journal of Geophysical Research 100 (D5), 8873–8892.
Herckes, P., Mirabel, P., Wortham, H., 2002a. Cloud water deposition at a high-elevation site in the Vosges Mountains (France). Science of the Total Environment 296 (1–3), 59–75.
Herckes, P., Wendling, R., Sauret, N., Mirabel, P., Wortham, H., 2002b. Cloudwater studies at a high elevation site in the Vosges Mountains (France). Environmental Pollution 117 (1), 169–177.
Hong, S.-Y., Dudhia, J., Chen, S.-H., 2004. A revised approach to ice microphysical processes for the bulk parameterization of clouds and precipitation. Monthly Weather Review 132, 103–120.
Hong, S.-Y., Lim, J.-O.J., 2006. The WRF single-moment 6-class microphysics scheme (WSM6). Journal of Korean Meteorological Society 42, 129–151.
Hong, S.-Y., Noh, Y., Dudhia, J., 2006. A new vertical diffusion package with an explicit treatment of entrainment processes. Monthly Weather Review 134, 2318–2341.
Ichikawa, Y., Hayami, H., Fujita, S., 1998. A long-range transport model for East Asia to estimate sulfur deposition in Japan. Journal of Applied Meteorology 37, 1364–1374. 10 PART II.
Igawa, M., Tsutsumi, Y., Mori, T., Okochi, H., 1998. Fogwater chemistry at a mountainside forest and the estimation of the air pollutant deposition via fog droplets based on the atmospheric quality at the mountain base. Environmental Science and Technology 32 (11), 1566–1572.
Kain, J.S., 2004. The Kain-Fritsch convective parameterization. An update. Journal of Applied Meteorology 43 (1), 170–181.
Kannari, A., Tonooka, Y., Baba, T., Murano, K., 2007. Development of multiple-species 1 km × 1 km resolution hourly basis emissions inventory for Japan. Atmospheric Environment 41 (16), 3428–3439.
Katata, G., Nagai, H., Wrzesinsky, T., Klemm, O., Eugster, W., Burkard, R., 2008. Development of a land surface model including cloud water deposition on vegetation. Journal of Applied Meteorology and Climatology 47 (8), 2129–2146.
Klemm, O., Wrzesinsky, T., Cheer, C., 2005. Fog water flux at a canopy top: direct measurement versus one-dimensional model. Atmospheric Environment 39 (29), 5375–5386.
Klemm, O., Wrzesinsky, T., 2007. Fog deposition fluxes of water and ions to a mountainous site in Central Europe. Tellus B 59 (4), 705–714.
Kondo, J., Akashi, S., 1976. Numerical studies on the two-dimensional flow in horizontally homogeneous canopy layers. Boundary-Layer Meteorology 10 (3), 255–272.
Lange, C.A., Matschullat, J., Zimmermann, F., Sterzik, G., Wienhaus, O., 2003. Fog frequency and chemical composition of fog water – a relevant contribution to atmospheric deposition in the eastern Erzgebirge, Germany. Atmospheric Environment 37 (26), 3731–3739.
Lee, S.-H., Kim, Y.-K., Kim, H.-S., Lee, H.-W., 2007. Influence of dense surface meteorological data assimilation on the prediction accuracy of ozone pollution in the southeastern coastal area of the Korean Peninsula. Atmospheric Environment 41 (21), 4451–4465.
Lin, M., Oki, T., Bengtsson, M., Kanae, S., Holloway, T., Streets, D.G., 2008. Long-range transport of acidifying substances in East Asia–part II. Source-receptor relationships. Atmospheric Environment 42 (24), 5956–5967.
Lovett, G.M., 1984. Rates and mechanisms of cloud water deposition to a subalpine balsam fir forest. Atmospheric Environment 18 (2), 361–371.
Mellor, G.L., Yamada, T., 1982. Development of a turbulence closure model for geophysical fluid problems. Reviews of Geophysics & Space Physics 20 (4), 851–875.
Mlawer, E.J., Taubman, S.J., Brown, P.D., Iacono, M.J., Clough, S.A., 1997. Radiative transfer for inhomogeneous atmospheres: RRTM, a validated correlated-k model for the longwave. Journal of Geophysical Research 102 (D14), 16663–16682.
Miller, E.K., Panek, J.A., Friedland, A.J., Kadlecek, J., Mohnen, V.A., 1993. Atmospheric deposition to a high-elevation forest at Whiteface Mountain, New York, USA. Tellus 45B (3), 209–227.
Murano, K., 2006. International Co-operative Survey to Clarify the Trans-boundary air Pollution Across the Northern Hemisphere (Abstract of the Final Report), Summary Report of Research Results under the GERF (Global Environment Research Fund) in FY2004, 237–243, Research and Information Office, Global Environment Bureau, Ministry of the Environment, Government of Japan.
Ohara, T., Akimoto, H., Kurokawa, J., Horii, N., Yamaji, K., Yan, X., Hayasaka, T., 2007. An Asian emission inventory of anthropogenic emission sources for the period 1980–2020. Atmospheric Chemistry and Physics 7 (16), 4419–4444.
Pagowski, M., Gultepe, I., King, P., 2004. Analysis and modeling of an extremely dense fog event in southern Ontario. Journal of Applied Meteorology 43 (1), 3–16.
Petroff, A., Zhang, L., Pryor, S.C., Belot, Y., 2009. An extended dry deposition model for aerosols onto broadleaf canopies. Journal of Aerosol Science 40 (3), 218–240.
Pleim, J.E., Chang, J., 1992. A non-local closure model for vertical mixing in the convective boundary layer. Atmospheric Environment 26A, 965–981.
Restad, K., Isaksen, I.S.A., Berntsen, T.K., 1998. Global distribution of sulphate in the troposphere. A three-dimensional model study. Atmospheric Environment 32 (20), 3593–3609.
Shimadera, H., Shrestha, K.L., Kondo, A., Kaga, A., Inoue, Y., 2008. Fog simulation using a mesoscale model in and around the Yodo River Basin, Japan. Journal of Environmental Sciences 20 (7), 838–845.
Shimadera, H., Kondo, A., Kaga, A., Shrestha, K.L., Inoue, Y., 2009. Contribution of transboundary air pollution to ionic concentrations in fog in the Kinki Region of Japan. Atmospheric Environment 43 (37), 5894–5907.
Shimadera, H., Kondo, A., Kaga, A., Shrestha, K.L., Inoue, Y., 2010. Numerical predictions of sulfur and nitrogen depositions through fog in forest areas. Journal of Japan Society for Atmospheric Environment 45 (6), 247–255.
Shubzda, J., Lindberg, S.E., Garten, C.T., Nodvin, S.C., 1995. Elevational trends in the fluxes of sulphur and nitrogen in throughfall in the Southern Appalachian Mountains: some suprising results. Water, Air, and Soil Pollution 85 (4), 2265–2270.
Skamarock, W.C., Klemp, J.B., Dudhia, J., Gill, D.O., Baker, D.M., Duda, M.G., Huang, X.-Y., Wang, W., Powers, J.G., 2008. A Description of the Advanced Research WRF Version 3 NCAR Technical Note, NCAR/TN-475+STR.
Stoelinga, M.T., Warner, T.T., 1999. Nonhydrostatic, mesobeta-scale model simulations of cloud ceiling and visibility for an East Coast winter precipitation event. Journal of Applied Meteorology 38 (4), 385–404.
Streets, D.G., Yarber, K.F., Woo, J.-H., Carmichael, G.R., 2003. Biomass burning in Asia: annual and seasonal estimates and atmospheric emissions. Global Biogeochemical Cycles 17 (4), 10/1–10/20.
Tsai, I.-C., Chen, J.-P., Lin, P.-Y., Wang, W.-C., Isaksen, I.S.A., 2010. Sulfur cycle and sulfate radiative forcing simulated from a coupled global climate-chemistry model. Atmospheric Chemistry and Physics 10 (8), 3693–3709.
U.S. EPA, 2008. AEROSOL_NOTES.txt. CMAQ v4.7 documentation.
Vermeulen, A.T., Wyers, G.P., Römer, F.G., Van Leeuwen, N.F.M., Draaijers, G.P.J., Erisman, J.W., 1997. Fog deposition on a coniferous forest in the Netherlands. Atmospheric Environment 31 (3), 375–386.
Vong, R.J., Sigmon, J.T., Mueller, S.F., 1991. Cloud water deposition to Appalachian forests. Environmental Science and Technology 25 (6), 1014–1021.
Wang, C., Corbett, J.J., Firestone, J., 2008. Improving spatial representation of global ship emissions inventories. Environmental Science and Technology 42 (1), 193–199.
Willmott, C.J., 1981. On the validation of models. Physical Geography 2 (2), 184–194.
Yamada, T., 1982. A numerical model study of turbulent airflow in and above a forest canopy. Journal of the Meteorological Society of Japan 60, 439–454.
Zhang, Q., Streets, D.G., Carmichael, G.R., He, K., Huo, H., Kannari, A., Klimont, Z., Park, I., Reddy, S., Fu, J.S., Chen, D., Duan, L., Lei, Y., Wang, L., Yao, Z., 2009. Asian emissions in 2006 for the NASA INTEX-B mission. Atmospheric Chemistry and Physics Discussions 9 (1), 4081–4139.

Please cite this article in press as: Shimadera, H., et al., Annual sulfur deposition through fog, wet and dry deposition in the Kinki Region of Japan, Atmospheric Environment (2011), doi:10.1016/j.atmosenv.2011.08.055